Journal of Molecular Modeling (2019) 25: 184
https://doi.org/10.1007/s00894-019-4081-9

ORIGINAL PAPER

Water-assisted peptide bond formation between two double amino acid molecules in the gas phase

Sylwia Freza[1]

Received: 21 February 2019 / Accepted: 28 May 2019 / Published online: 7 June 2019

Abstract

The gas phase mechanism of the peptide bond formation between two double amino acid (DAA) molecules described by the $(NH_2)_2C(COOH)_2$ formula is investigated in the presence of a water molecule. Formations of *trans* and *cis* DAA–DAA dipeptide products along both concerted and stepwise mechanisms have been studied at the CCSD(T)/aug-cc-pVDZ//MP2/aug-cc-pVDZ level. The results indicate that the activation energy barriers estimated for the water-assisted mechanisms are significantly reduced in comparison to the corresponding uncatalyzed reactions. The *trans* DAA–DAA isomer is expected to dominate in the final product due to its larger stability compared to the *cis* DAA–DAA product.

Keywords Double amino acid · Peptide bond · Ab initio calculations

Introduction

Condensation of amino acids is a crucial reaction in protein chemistry as it represents a key reaction for all life processes. An essential structural element of all proteins is a peptide bond (C–N), which is formed because of the conjugation between the α-amino group of one amino acid and the α-carboxylic group of another amino acid. The detailed knowledge of the peptide bond formation mechanism is vital for understanding of various biological processes, and it is a subject of intensive investigations as such. The uncatalyzed reaction of peptide bond formation has been studied by Oie et al. [1] and Jensen et al. [2], who predicted two possible mechanisms, namely concerted and stepwise, and summarized that these two routes may compete since both require similar activation energies (relative energies of the highest transition state structure with respect to the reactants are about 40–47 kcal mol^{-1}). More recently, similar results have been obtained by Redondo et al. [3] and Dornshuld et al. [4], who performed the investigation of glycine condensation in the absence of any catalysts.

Typical high-yielding reactions of peptide bond formation require the presence of an activated amino acid precursor [5]. On the other hand, the synthesis of peptide bond by direct condensation of unactivated amino acids is a very slow process, and the presence of a suitable catalyst is needed in order to overcome kinetic limitation [6]. The catalytic role in the formation of polypeptides can be played by minerals [7], mineral and metal oxide surfaces [8–11], metal dications (e.g., Mg^{2+}, Ca^{2+}, Cu^{2+} or Ni^{2+}) [12–16], and protic solvents (such as ammonia [17] and water [18]). Theoretical calculations have also been proven useful in this field as providing an insight into such mechanisms at the molecular level. For example, Oie et al. [19] employed computational methods to study the amine catalyzed peptide bond formation between formic acid and an ammonia molecule and demonstrated that the activation barrier was reduced by about 10 kcal mol^{-1} with respect to the uncatalyzed process. Even more promising results were obtained by Rimola et al., who theoretically investigated the effect of the simultaneous presence of Lewis and Brønsted catalysts (AlF_3 and HF, respectively) on the same reaction. Namely, they found that the synergy between these catalysts reduces the activation energy barrier from 56.0 kcal mol^{-1} (uncatalyzed reaction) to 14.4 kcal mol^{-1} [20]. Since the water molecules are generated during the amino acids condensation, earlier computational studies were also focused on the catalytic role that H_2O plays in the Ala–Ala peptide bond formation [18] and on the generation of cyclic dipeptide from various amino acids [21]. In both these cases, the barrier heights were found to be systematically reduced owing to the assistance of water molecules. The same effect was

✉ Sylwia Freza
sylwia.freza@ug.edu.pl

[1] Laboratory of Quantum Chemistry, Faculty of Chemistry, University of Gdańsk, Wita Stwosza 63, 80-308 Gdańsk, Poland

observed for very similar process, namely the ammonia addition to formaldehyde assisted by water, which has been investigated by Williams [22].

In this contribution, we explore the gas phase mechanism of the peptide bond formation between two double amino acid (DAA) molecules in the presence of a water molecule. The double amino acid (described by the $(NH_2)_2C(COOH)_2$ formula, see Fig. 1) has been recently proposed by our group as a novel amino acid enabling peptide interpenetrating structures [23]. Its stability with respect to both unimolecular deamination and decarboxylation reactions has already been addressed in order to show that spontaneous detachment of either ammonia or the carbon dioxide molecule in gas and aqueous phases is not operative [24, 25]. Moreover, we demonstrated that the DAA system acts similarly to various natural amino acids when the noncatalyzed peptide bond formation process between two DAA molecules or the cyclization involving two DAAs in gas phase are considered [26, 27].

Since the formation of each peptide bond is accompanied by the release of a water molecule, the main goal of this contribution is to verify how the presence of H_2O molecules affects the condensation of two DAA systems.

Computational methods

The structures of the reactants, transition states, intermediate and final products were optimized by employing the second–order Møller–Plesset perturbational method (MP2) [28–30] with the aug-cc-pVDZ basis set [31–33]. The analytical calculations of harmonic vibrational frequencies computed at the same level of theory allowed verification of the nature of all stationary points and thereby they were identified as either minima (no imaginary frequency) or first order saddle (one imaginary frequency). For each transition state structure, we carried out the intrinsic reaction coordinate (IRC) calculations [34–36] in both forward and reverse directions at the same MP2/aug-cc-pVDZ level of theory. The electronic energies of all stationary points were then refined by employing the CCSD(T) method (coupled-cluster method with single and double excitations augmented with noniterative triple excitations) [37, 38] using the same aug-cc-pVDZ basis set.

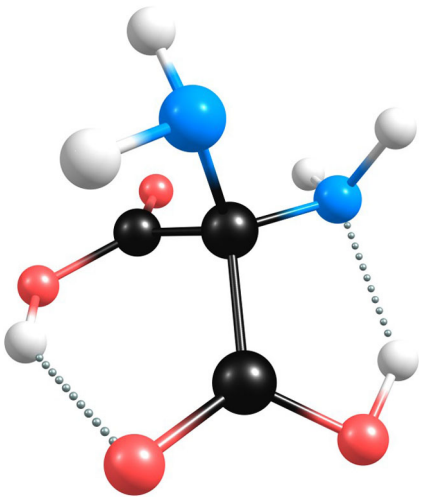

Fig. 1 Equilibrium structure of the most stable canonical isomer of double amino acid (DAA) molecule in the gas phase

Transition state theory [39] was used to obtain rate constants (k_{298}) for the investigated reaction ($k_{298} = {}^{kT}/_{h} exp^{{}^{-\Delta G^{\#}}/_{RT}}$) where k is the Boltzmann constant, T is the temperature (298.15 K), and h stands for Planck's constant. The Gibbs free energies ($\Delta G^{\#}$) of the transition states were evaluated using the CCSD(T)/aug-cc-pVDZ electronic energies, while the entropy contributions, zero-point-energy corrections, and thermal corrections (at T = 298.15 K) were estimated at the MP2/aug-cc-pVDZ theory level.

All calculations were performed using the Gaussian16 program package [40], whereas the the Chemcraft program [41] was utilized to visualize the equilibrium structures of all compounds.

While performing our calculations, we assumed that the starting reactants consist of two DAA molecules in their canonical forms (i.e., containing two NH_2 and two COOH groups intact) and a single water molecule.

Results and discussion

The reaction mechanisms studied in this contribution and related to the water-assisted peptide bond formation between two DAA molecules are depicted in Figs. 2, 3, 4, and 5 together with relative energies of all systems involved. As mentioned in the preceding section, the canonical forms of DAA molecules (see Fig. 1) have been chosen as the starting reactants due to their highest stability in the gas phase.

Concerted mechanisms

The mechanisms presented in Figs. 2 and 3 correspond to the reaction paths leading to DAA–DAA dipeptide containing its peptide bond in either *trans* or *cis* configuration, respectively. Since in both cases the reactants and products are connected by only one transition state (**TS**) structure, these mechanisms can be considered as concerted. The initial step in both reactions involves a formation of the reactant complex (**RC**) whose energy is lower than that of the noninteracting substrates by 21.2 kcal mol^{-1}. Clearly, the **RC** gains its stability due to formation of intra- and inter-molecular hydrogen bonds depicted in Figs. 2 and 3. The analysis of both concerted mechanisms reveals that the peptide bond is formed through a transition state structure containing a six-membered ring

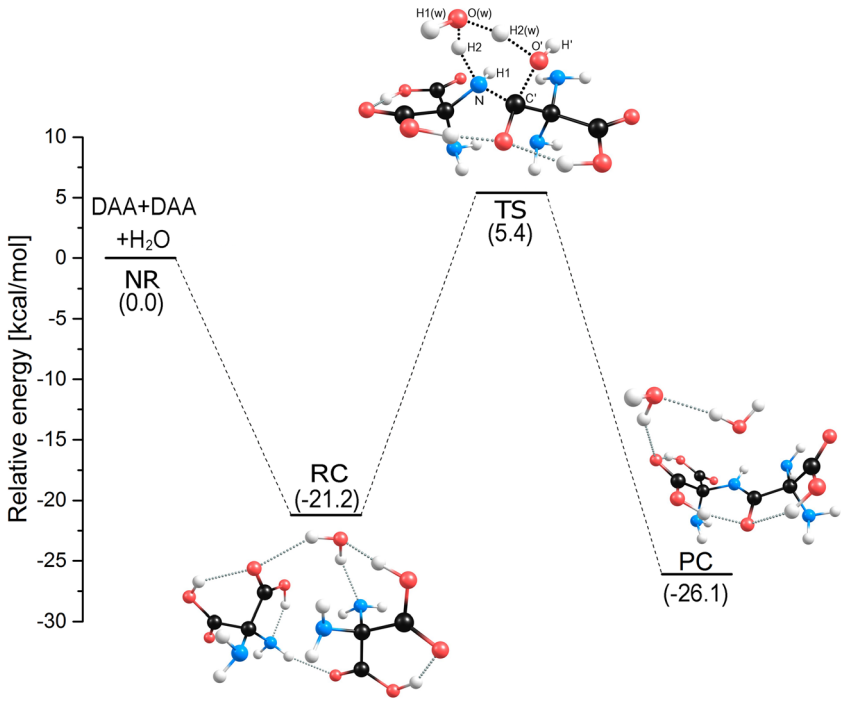

Fig. 2 Energy profile for the water assisted peptide bond formation between two double amino acid molecules according to the concerted mechanism and leading to the *trans* DAA–DAA. Relative energies (in kcal mol^{-1}) of the stationary points were obtained at the CCSD(T)/aug-cc-pVDZ//MP2/aug-cc-pVDZ level of theory (the energy of the noninteracting reacants was taken as zero)

involving a water molecule (unlike the highly strained four-membered ring **TS** structures found earlier for the corresponding noncatalyzed concerted mechanisms [27]). It is important to notice that in these two **TS** structures (for which the imaginary vibration frequencies are equal to 837i cm^{-1} and 630i cm^{-1} for the *trans* and *cis* route, respectively) the water molecule acts as both a hydrogen atom acceptor and donor with respect to the amino group of one DAA and the OH group of the second DAA molecule. This intermolecular hydrogen transfer where atom H2 goes to the atom O(w) and simultaneously atom H2(w) belonging to the water molecule migrates to oxygen atom O′ is accompanied by the C′–O′ bond cleavage and leads to the elimination of the H_2O molecule (see the **TS** structures depicted in Figs. 2 and 3). The calculated energy barrier that has to be surmounted in this step for the route leading to the *trans* product is equal to 26.6 kcal mol^{-1} (the related rate constant $k_{(ct)}$ is equal to 5.43×10^{-3} s^{-1}), whereas the corresponding barrier predicted for the path leading to the

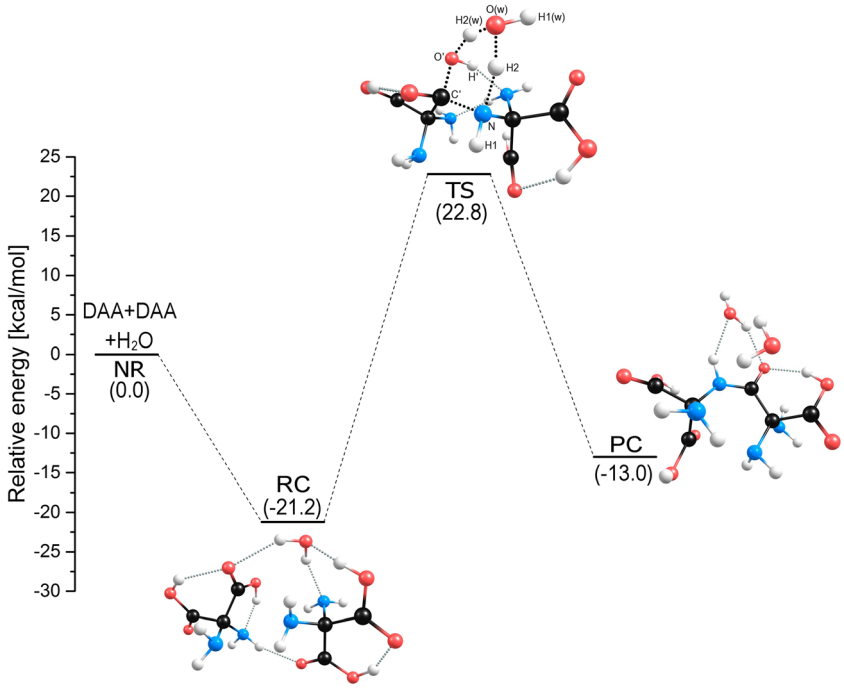

Fig. 3 Energy profile for the water assisted peptide bond formation between two double amino acid molecules according to the concerted mechanism and leading to the *cis* DAA–DAA. Relative energies (in kcal mol^{-1}) of the stationary points were obtained at the CCSD(T)/aug-cc-pVDZ//MP2/aug-cc-pVDZ level of theory (the energy of the noninteracting reacants was taken as zero)

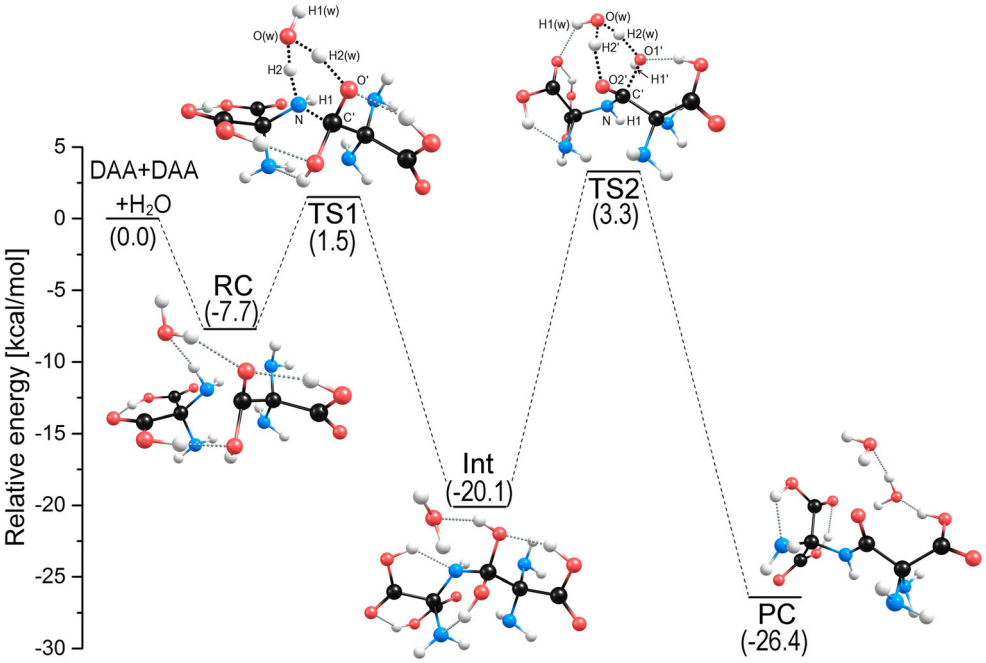

Fig. 4 Energy profile for the water assisted peptide bond formation between two double amino acid molecules according to the stepwise mechanism and leading to the *trans* DAA–DAA. Relative energies (in kcal mol^{-1}) of the stationary points were obtained at the CCSD(T)/aug-cc-pVDZ//MP2/aug-cc-pVDZ level of theory (the energy of the noninteracting reacants was taken as zero)

cis structure is much larger and equals 44.0 kcal mol^{-1} (the related rate constant $k_{(cc)}$ is equal to 2.26×10^{-15} s^{-1}). After passing the saddle point, the final product corresponding to the DAA–DAA is formed. Depending on the mechanism considered, the resulting dipeptide contains its peptide bond in either *trans* or *cis* configuration. Since the presence of one H_2O molecule (playing the catalyst role) was initially assumed and taking into account that the formation of a single peptide bond results in elimination of another H_2O molecule, the interaction of such three systems has to be considered to assure consistency of the energy profile investigated. As it turns out, the lowest energy final structure (i.e., "product complex" labeled **PC** in Figs. 2 and 3) corresponds to the complex of two water molecules and either a *trans* or *cis* DAA–DAA isomer.

As shown in Figs. 2 and 3, the process of peptide bond formation between two DAA molecules with the assistance

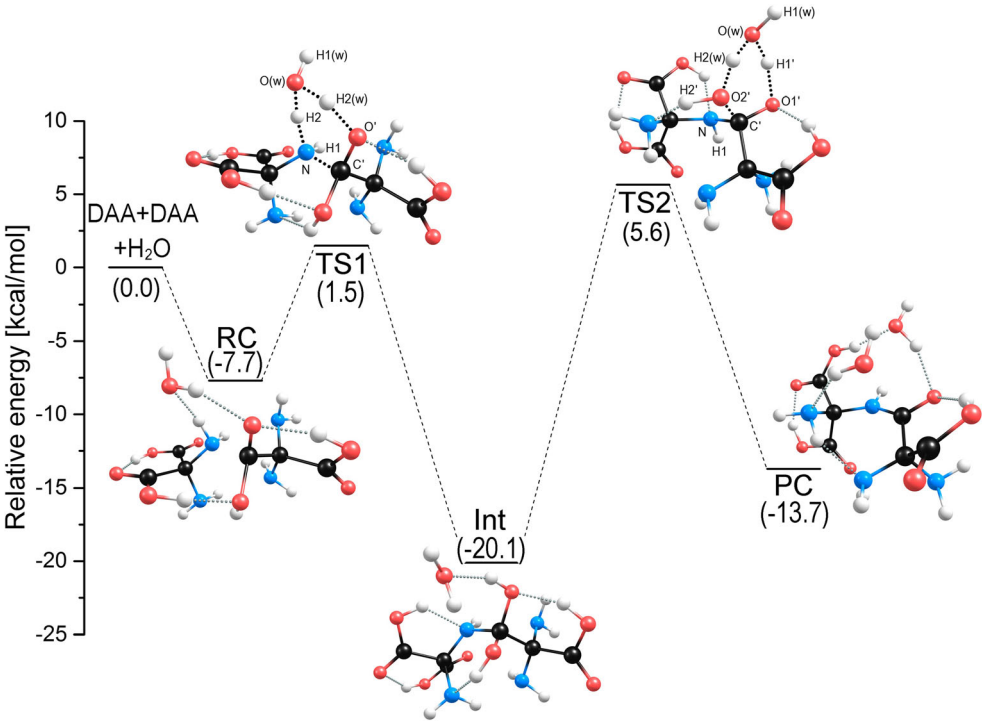

Fig. 5 Energy profile for the water assisted peptide bond formation between two double amino acid molecules according to the stepwise mechanism and leading to the *cis* DAA–DAA. Relative energies (in kcal mol^{-1}) of the stationary points were obtained at the CCSD(T)/aug-cc-pVDZ//MP2/aug-cc-pVDZ level of theory (the energy of the noninteracting reacants was taken as zero)

of a water molecule and undergoing the concerted mechanism is energetically favorable by 26.1 kcal mol^{-1} (when the *trans* DAA–DAA is formed) or 13.0 kcal mol^{-1} (when the *cis* DAA–DAA is the final product). However, one may notice that the initial reactant complex is actually lower in energy than the final complex involving *cis* DAA–DAA and two water molecules (see Fig. 3), hence the route leading to the *cis* DAA–DAA should not be considered plausible. Moreover, the height of the activation barrier for this path (44.0 kcal mol^{-1}) also seems to be too large to render this route operative. On the other hand, the final complex of *trans* DAA–DAA and two water molecules (see **PC** in Fig. 2) represents the lowest energy structure on the corresponding energy profile as its energy is smaller than that of the initial reactant complex (**RC** in Fig. 2) by ca. 5 kcal mol^{-1}. Also the height of the activation barrier for the formation of *trans* DAA–DAA (26.6 kcal mol^{-1}) indicates that this path can be considered operative.

Therefore, we conclude that only the *trans* DAA–DAA dipeptide can be generated according to the concerted mechanism predicted for the water-assisted peptide bond formation between two DAA species due to both thermodynamical stability thereof with respect to the reactant complex (the final complex of *cis* DAA–DAA and two water molecules is higher in energy than the corresponding **RC** complex) and significantly lower activation barrier that has to be surmounted compared to the *trans* pathway.

Stepwise mechanisms

Our calculations indicate that the water-assisted DAA–DAA dipeptide formation may alternatively proceed according to the stepwise mechanism. The energy profiles corresponding to the reactions leading to *trans* and *cis* dipeptide are shown in Figs. 4 and 5, respectively. The initial step in both processes is the formation of the hydrogen bonded reactant complex (**RC**). It should be noted, however, that the **RC** structure presented in Figs. 4 and 5 (i.e., for the stepwise route) is actually different than the **RC** shown in Figs. 2 and 3 (i.e., for the concerted route) because in both cases the **RC** local minimum energy structure was found by employing the IRC calculations and matches its corresponding transition state as such. In particular, the reactant complex predicted for the stepwise mechanisms consists of two DAA amino acids connected together via the H-bonds and H_2O molecule whose oxygen and hydrogen atoms form hydrogen bonds with functional groups of both DAAs (see **RC** structure in Figs. 4 and 5). The resulting H-bond network renders this reactant complex stable with respect to the noninteracting substrates by 7.7 kcal mol^{-1}. In the next step, the **RC** passes through the energy barrier of 9.2 kcal mol^{-1} (the corresponding rate constant $k_{(s1)}$ is equal to 2.13×10^9 s^{-1}) via the transition state structure (labeled **TS1** in Figs. 4 and 5) to form the intermediate product (**Int**). The analysis of both the saddle point structure and the imaginary vibration mode (υ = 1383i cm^{-1}) reveals that the peptide C′–N bond is formed during this step by the nucleophilic attack of the N atom of the NH_2 group of one double amino acid molecule to the C′ atom of the carboxylic group available in the second DAA. In addition, the hydrogen H2 migrates from the NH_2 group to the oxygen atom of the water molecule O(w) with simultaneous transfer of the second hydrogen atom H2(w) from the water molecule to O′ oxygen atom belonging to the second DAA. The energy profiles show that the resulting intermediate product (**Int**) is more stable than the reactants by 20.1 kcal mol^{-1}. It is also important to emphasize that the C′–N bond is already formed in the **Int** structure.

Once this intermediate product structure is achieved, the two routes become possible, leading either to the *trans* DAA–DAA or to the *cis* DAA–DAA product. The reaction resulting in the formation of *trans* DAA–DAA requires passing the energy barrier of 23.4 kcal mol^{-1} and proceeds through the **TS2** transition state (the corresponding rate constant $k_{(s2t)}$ is equal to 2.6 s^{-1}). Analysis of the imaginary frequency mode (596i cm^{-1}) shows that during this process, the hydrogen atom migrates (through the assisting water molecule) between two OH groups connected to the same carbon atom in the **Int** structure, namely the H2' atom goes to the O(w) oxygen atom and the H2(w) hydrogen atom transfers to the O1' oxygen. This process is accompanied by the C′–O1' bond cleavage and elimination of another H_2O system, see the **TS2** and **Int** structures depicted in Fig. 4. The final product (**PC**) formed along this path represents the *trans* DAA–DAA dipeptide interacting with the water dimer and the energy of this complex is lower than that of the starting reactants by 26.4 kcal mol^{-1}. Alternatively, the intermediate product **Int** might evolve to the DAA–DAA containing its peptide bond in the *cis* configuration, see Fig. 5. Although the energy barrier that has to be overcome in that case is equal to 25.7 kcal mol^{-1} (which leads to the rate constant $k_{(s2c)}$ of 6.75 s^{-1}) and was predicted to be slightly higher than that found for the route leading to the *trans* DAA–DAA, the analysis of the **TS2** transition state structure and the imaginary vibration mode (1026i cm^{-1}) leads to similar conclusions. Namely, the hydrogen atom H1' is being transferred to the assisting water molecule with simultaneous migration of the H2(w) atom to the O2' oxygen, which is accompanied by the C′–O2' bond rupture and elimination of another H_2O, see Fig. 5. In fact, the **TS2** structures predicted for the paths leading to *trans* and *cis* dipeptide and depicted in Figs. 4 and 5 differ only by mutual orientation of two amino acids and the water molecule, which enables the formation of the DAA–DAA containing its peptide bond in various configurations. The final product on the path leading to the *cis* DAA–DAA represents the complex of

the dipeptide interacting with two water molecules, and its energy is lower by 13.7 kcal mol^{-1} than the energy of the reactants.

The comparison of the energy profiles predicted for two stepwise mechanisms and given in Figs. 4 and 5 reveals that the energy barriers that have to be surmounted are similar for both paths (although the second barrier is slightly smaller for the route leading to the *trans* DAA–DAA), whereas the energies of the final product complexes differ significantly (i.e., the **PC** including *trans* dipeptide is more stable by 12.7 kcal mol^{-1} than that including the *cis* dipeptide). Clearly, this difference is mainly caused by the larger stability of *trans* in comparison to *cis* DAA–DAA isomer and also by different H-bond networks formed by each of these structures with two water molecules.

Thus, we conclude that the water-assisted peptide bond formation between two DAA molecules according to the stepwise mechanisms should lead to both *trans* and *cis* isomers of DAA–DAA; however, the former isomer is expected to dominate in the bulk.

Conclusions

The formation of *trans* and *cis* peptide bonds (C–N) between two double amino acids catalyzed by a single H_2O molecule and proceeding along either concerted or stepwise paths have been studied at the CCSD(T)/aug-cc-pVDZ//MP2/aug-cc-pVDZ level of theory. The results obtained for the concerted mechanisms reveal that only the path leading to the *trans* DAA–DAA should be considered operative, whereas a relatively large energy barrier and large stability of the initial complex render the formation of *cis* DAA–DAA not plausible. On the other hand, the formation of both *trans* and *cis* isomers seems likely when the stepwise paths are concerned. In any case, the *trans* DAA–DAA isomers are expected to dominate in the final product due to the smaller energy barriers on the paths leading to these conformers and because of larger stability of the *trans* DAA–DAA structure. Recalling that the *trans* conformation of the peptide bond is typically favored in most peptide structures due to the smaller steric repulsion between the two Cα atoms (the Cα–C–N–Cα dihedral angle approaches 180° in *trans* and 0° in *cis* conformation), whereas the *cis* peptide bond occurs more frequently only when the proline residue is involved [42–44], we conclude that the peptide bond of *trans* configurations should also be preferred when formed by DAAs.

The presence of a water molecule during the formation of DAA–DAA dipeptide has been proven important regardless of the conformation of the final product as the energy barriers predicted for the water-assisted mechanisms are significantly reduced in comparison to the barriers found for the corresponding uncatalyzed reactions [27]. In order to explain the catalytic role of the H_2O molecule in this process, one may follow the speculation provided in ref. [45] based on the comparison of the stability of four- vs six-membered rings. Namely, the steric strain existing in the four-membered ring transition state structures (that are characterized in the uncatalyzed mechanisms) likely raises the energies of those systems. By contrast, in the water assisted mechanisms, the transition state structures involve six-membered rings with smaller strain and thus higher stability.

Acknowledgments This research was supported by the Polish Ministry of Science and Higher Education grant No. DS 530-8375-D499-19. The calculations have been carried out using resources provided by Wroclaw Centre for Networking and Supercomputing (http://wcss.pl) grant No. 436.

References

1. Oie T, Loew GH, Burt SK, Binkley JS, MacElroy RD (1982) J Am Chem Soc 104(23):6169–6174. https://doi.org/10.1021/ja00387a001
2. Jensen JH, Baldridge KK, Gordon MS (1992) J Phys Chem 96(21):8340–8351. https://doi.org/10.1021/j100200a025
3. Redondo P, Martínez H, Cimas Á, Barrientos C, Largo A (2013) Phys Chem Chem Phys 15(31):13005–13012. https://doi.org/10.1039/c3cp51535d
4. Van Dornshuld E, Vergenz RA, Tschumper GS (2014) J Phys Chem B 118(29):8583–8590. https://doi.org/10.1021/jp504924c
5. Montalbetti CAGN, Falque V (2005) Tetrahedron 61(46):10827–10852. https://doi.org/10.1016/j.tet.2005.08.031
6. Berg J, Tymoczko J, Stryer L (2002) Bicochemistry. Freeman, New York
7. Georgelin T, Jaber M, Bazzi H, Lambert JF (2013) Orig Life Evol Biosph 43(4–5):429–443. https://doi.org/10.1007/s11084-013-9345-2
8. Shanker U, Bhushan B, Bhattacharjee G, Kamaluddin (2012) Orig Life Evol Biosph 42(1):31–45. https://doi.org/10.1007/s11084-012-9266-5
9. Rimola A, Tosoni S, Sodupe M, Ugliengo P (2006) ChemPhysChem 7(1):157–163. https://doi.org/10.1002/cphc.200500401
10. Basiuk VA, Sainz-Rojas J (2001) Adv Sp Res 27(2):225–230. https://doi.org/10.1016/S0273-1177(01)00051-5
11. Bujdák J, Rode BMJ (2002) Inorg Biochem 90(1–2):1–7. https://doi.org/10.1016/S0162-0134(02)00395-1
12. Oie T, Loew GH, Burt SK, MacElroy RD (1984) J Am Chem Soc 106(26):8007–8013. https://doi.org/10.1021/ja00338a001
13. Yamagata Y, Inomata K (1997) Orig Life Evol Biosph 27(4):339–344. https://doi.org/10.1023/A:1006529421813
14. Rode BM, Suwannachot Y (1999) Coord Chem Rev 190–192:1085–1099. https://doi.org/10.1016/S0010-8545(99)00159-9

15. Rimola A, Rodríguez-Santiago L, Ugliengo P, Sodupe M (2007) J Phys Chem B 111(20):5740–5747. https://doi.org/10.1021/jp071071o
16. Remko M, Michael B (2001) Phys Chem Chem Phys 3:4667–4673. https://doi.org/10.1039/b105623a
17. Oie T, Loew GH, Burt SK, Binkley JS, MacElroy RD (1982) Int J Quantum Chem 22(9 S):223–245. https://doi.org/10.1002/qua.560220722
18. Thirumoorthy K, Nandi N (2007) J Mol Struct Theochem 818(1–3):107–118. https://doi.org/10.1016/j.theochem.2007.05.017
19. Oie T, Loew GH, Burt SK, MacElroy RD (1983) J Am Chem Soc 105(8):2221–2227. https://doi.org/10.1021/ja00346a020
20. Rimola A, Tosoni S, Sodupe M, Ugliengo P (2005) Chem Phys Lett 408(4–6):295–301. https://doi.org/10.1016/j.cplett.2005.04.056
21. Li Y, Li F, Zhu Y, Li X, Zhou Z, Liu C, Zhang W, Tang M (2016) Struct Chem 27(4):1165–1173. https://doi.org/10.1007/s11224-016-0740-y
22. Williams IH (1987) J Am Chem Soc. https://doi.org/10.1021/ja00255a012
23. Freza S, Marchaj M, Skurski P (2014) Chem Phys Lett 599:34–37. https://doi.org/10.1016/j.cplett.2014.03.020
24. Freza S (2017) Theor Chem Accounts 136:7. https://doi.org/10.1007/s00214-016-2031-5
25. Freza S (2016) Theor Chem Accounts 135:146. https://doi.org/10.1007/s00214-016-1906-9
26. Freza S (2018) Struct Chem 29(4):1025–1029. https://doi.org/10.1007/s11224-018-1085-5
27. Czapla M, Freza S (2017) Int J Quantum Chem 117(21):e25435. https://doi.org/10.1002/qua.25435
28. Møller C, Plesset MS (1934) Phys Rev 46(7):618–622. https://doi.org/10.1103/PhysRev.46.618
29. Head-Gordon M, Pople JA, Frisch M (1988) J Chem Phys Lett 153(6):503–506. https://doi.org/10.1016/0009-2614(88)85250-3
30. Frisch MJ, Head-Gordon M, Pople JA (1990) Chem Phys Lett 166(3):275–280. https://doi.org/10.1016/0009-2614(90)80029-D
31. Dunning Jr THJ (1989) Chem Phys. https://doi.org/10.1063/1.456153
32. Kendall RA, Dunning TH, Harrison RJJ (1992) Chem Phys 96(9):6796–6806. https://doi.org/10.1063/1.462569
33. Woon DE, Dunning THJ (1993) Chem Phys 98(2):1358–1371. https://doi.org/10.1063/1.464303
34. Hratchian HP, Schlegel HBJ (2004) Chem Phys 120(21):9918–9924. https://doi.org/10.1063/1.1724823
35. Hratchian HP, Schlegel HB (2005) J Chem Theory Comput 1(1):61–69. https://doi.org/10.1021/ct0499783
36. Fukui K (1981) Acc Chem Res 14(12):363–368. https://doi.org/10.1021/ar00072a001
37. Purvis GD, Bartlett RJJ (1982) Chem Phys 76(4):1910–1918. https://doi.org/10.1063/1.443164
38. Bartlett RJ, Purvis GD (1978) Int J Quantum Chem 14(5):561–581. https://doi.org/10.1002/qua.560140504
39. Lowry TH, Richardson K (1981) Mechanism and theory in organic chemistry, 2nd edn. Harper & Row, New York
40. Frisch MJ, Trucks GW, Schlegel HB, Scuseria GE, Robb MA, Cheeseman JR, Scalmani G, Barone V, Petersson GA, Nakatsuji H et al. (2016) Gaussian 16, revision B.01. Gaussian Inc, Wallingford
41. Chemcraft- graphical software for visualization of quantum chemistry computations. https://www.chemcraftprog.com
42. Grathwohl C, Wüthrich K (1976) Biopolymers 15(10):2025–2041. https://doi.org/10.1002/bip.1976.360151012
43. Brandts JF, Halvorson HR, Brennan M (1975) Biochemistry 14(22):4953–4963. https://doi.org/10.1021/bi00693a026
44. Juy M, Lam-Thanh H, Lintner K, Fermandjian S (1983) Int J Pept Protein Res 22(4):437–449. https://doi.org/10.1111/j.1399-3011.1983.tb02113.x
45. Carey FA, Sundberg RJ (2007) Advanced organic chemistry part A. https://doi.org/10.1021/ed065pA139.2